

Standardization of choroidal thickness measurements using enhanced depth imaging optical coherence tomography

Nattapon Boonarpa^{1,2}, Yalin Zheng^{1,2}, Alexandros N. Stangos², Huiqi Lu^{1,2}, Ankur Raj^{1,2}, Gabriela Czanner^{1,3}, Simon P. Harding^{1,2}, Jayashree Nair-Sahni^{1,2}

¹Department of Eye and Vision Science, Institute of Ageing and Chronic Disease, University of Liverpool, Liverpool L69 3GA, United Kingdom

²St. Paul's Eye Unit, Royal Liverpool University Hospital, Liverpool L7 8XP, United Kingdom

³Department of Biostatistics, University of Liverpool, Liverpool L69 3GS, United Kingdom

Correspondence to: Jayashree Nair-Sahni. Department of Eye and Vision Science, Institute of Ageing and Chronic Disease, University of Liverpool, 3rd Floor, UCD Building, Daulby Street, Liverpool L69 3GA, United Kingdom. j.sahni@liverpool.ac.uk

Received: 2014-11-01

Accepted: 2014-12-15

Abstract

• **AIM:** To describe and evaluate a standardized protocol for measuring the choroidal thickness (ChT) using enhanced depth imaging optical coherence tomography (EDI OCT).

• **METHODS:** Single 9 mm EDI OCT line scans across the fovea were used for this study. The protocol used in this study classified the EDI OCT images into four groups based on the appearance of the choroidal-scleral interface and suprachoroidal space. Two evaluation iterations of experiments were performed: first, the protocol was validated in a pilot study of 12 healthy eyes. Afterwards, the applicability of the protocol was tested in 82 eyes of patients with diabetes. Inter-observer and intra-observer agreements on image classifications were performed using Cohen's kappa coefficient (κ). Intraclass correlation coefficient (ICC) and Bland-Altman's methodology were used for the measurement of the ChT.

• **RESULTS:** There was a moderate ($\kappa=0.42$) and perfect ($\kappa=1$) inter- and intra-observer agreements on image classifications from healthy eyes images and substantial ($\kappa=0.66$) and almost perfect ($\kappa=0.86$) agreements from diabetic eyes images. The proposed protocol showed excellent inter- and intra-observer agreements for the ChT measurements on both, healthy eyes and diabetic eyes (ICC >0.90 in all image categories). The Bland-

Altman plot showed a relatively large ChT measurement agreement in the scans that contained less visible choroidal outer boundary.

• **CONCLUSION:** A protocol to standardize ChT measurements in EDI OCT images has been developed; the results obtained using this protocol show that the technique is accurate and reliable for routine clinical practice and research.

• **KEYWORDS:** choroid; enhanced depth imaging; choroidal thickness; optical coherence tomography; diabetes

DOI:10.3980/j.issn.2222-3959.2015.03.09

Boonarpa N, Zheng Y, Stangos AN, Lu H, Raj A, Czanner G, Harding SP, Nair-Sahni J. Standardization of choroidal thickness measurements using enhanced depth imaging optical coherence tomography. *Int J Ophthalmol* 2015;8(3):484-491

INTRODUCTION

There is a growing interest in the role of the choroid in various chorioretinal diseases. Abnormalities of the choroidal integrity have been associated with the pathogenesis of several retinal diseases, such as age-related macular degeneration (AMD)^[1], central serous chorioretinopathy (CSCR)^[2] and diabetic maculopathy^[3].

New optical coherence tomography (OCT) image modalities, including enhanced depth imaging OCT (EDI OCT)^[4] and a longer wavelength swept source OCT^[5], enable a better visualization of the choroid in contrast to conventional techniques such as indocyanine green angiography and ultrasonography. Measuring the choroidal thickness (ChT) may become one of the determinants in the pathogenesis of several eye disease conditions^[2,6-8] as well as in healthy eyes during the aging process^[9-11].

The precise location of the choroidal-scleral interface (CSI) is essential for the accurate measurement of the ChT. Histologically, the choroid consists of 4 layers: Bruch's membrane, choriocapillaris, choroidal stroma and suprachoroid, which consists of the suprachoroidal lamina and the suprachoroidal space (SCS)^[12]. These choroidal histological structures are not clearly demarcated on the OCT images. Usually, the anterior boundary of the choroid is

easily identifiable in normal OCT and EDI OCT images as the outer limit of the hyper-reflective band representing the retinal pigment epithelium (RPE) and Bruch's membrane complex. The outer boundary of the choroid, on the other hand, appears to vary depending on the image quality. On EDI OCT images, the outer boundary of the choroid has been previously described by Spaide *et al*^[4] as the hypo-reflective space underneath the choroid SCS while Maul *et al*^[13] described it as a well demarcated hyper-reflective band between the large choroidal vessels and the sclera CSI. However, the clarity of the outer boundary of the choroid on EDI OCT images often suffer from the limitations of the penetration power of the OCT device and it might be further affected by the status and types of disease. This limitation may prevent the ability to visualize the choroidal structures on the EDI OCT images, resulting in the variability of manual measurements of the ChT, which in turn limit the applicability of EDI OCT measurements to identify and monitor pathology.

Different groups have defined the posterior boundary of the choroid as either the inner surface of the sclera or as the area demarcated by the hyper-reflective margin between the end of large choroidal vessels and the sclera^[9,10,14,15]. To date, there is a lack of clarity in the definition of the outer boundary of the choroid in ChT measurements which in turn may lead to problems in comparative studies.

In this study, we propose a standardized protocol for defining the variation in the topographical appearance of the choroidal posterior boundary in patients with eye disease using diabetes as a disease model. We have validated this standardized protocol by determining the inter- and intra-observer agreements in the classification of EDI OCT images and the inter- and intra-observer agreements of ChT measurements.

SUBJECTS AND METHODS

Subjects Subjects, including normal healthy volunteers with no known previous eye diseases and patients with diabetes, were recruited into this cross-sectional prospective observational study. The study was conducted in accordance with the Declaration of Helsinki. Informed consents were obtained from all subjects prior to their participation in the study.

All subjects underwent slit lamp biomicroscopy, best corrected visual acuity (BCVA) test using Bailey-Lovie logMAR (logarithm of the minimum angle of resolution) chart and EDI OCT scan on the Spectralis SD OCT system (Heidelberg Engineering, Heidelberg, Germany). For patients with diabetes, the inclusion criteria were men and women aged 18 or over with Type 1 or 2 diabetes mellitus, with or without any stage of diabetic retinopathy (DR). The degrees of retinopathy and maculopathy were graded by trained graders using the Liverpool Diabetic Eye Study (LDES) grading protocol^[16]. The exclusion criteria for patients with

diabetes included pregnancy, previous macular or pan-retinal laser treatment, contraindication to dilatation, history of intraocular injection or surgery and other significant eye diseases.

Horizontal EDI OCT images were taken using the Spectralis SD OCT system (Heidelberg Engineering, Heidelberg, Germany) by an externally accredited imaging scientist (Lu H). The EDI acquisition was done using the protocol previously described by Margolis and Spaide^[10]. An automatic real-time (ART) averaging of 100 was applied to each section using the built-in automatic averaging and real time eye-tracking features in order to obtain images of adequate quality for visualization and to maximize the signal-to-noise ratio. The images were exported at a 1:1 pixel ratio for analyses.

Standardized Protocol for Defining Choroidal Margins

Single 9 mm horizontal EDI OCT line scan passing through the center of the fovea was used for analysis. The foveal center was defined as the point of maximum depression within an area of 500 μm in diameter^[17]. When both the SCS and the CSI were identified in the image, the CSI was seen as a clear intermediate hyper-reflective band outer to the vascular-like structure of the choroid and the SCS was seen as a hypo-reflective band posterior to the CSI (Figure 1). The images were first classified into four sub-groups depending on the presence or the absence of the SCS and the CSI at the posterior boundary of the choroid (Figure 2).

Group A: both structures (CSI and SCS) were present and more than 80% of the CSI and SCS layers were identifiable across the length of the scan. Group B: 2 image categories were included within this group 1) both structures (CSI and SCS) were observed in the scan, however, it was in less than 80% of the length of the scan; 2) scans where only one of the structures were observed, either CSI or SCS. Group C: neither SCS nor CSI were observed in the scan, however, a distinct smooth line indicating the outer limit of the large choroidal vessels with the sclera was seen. Ungradable: scans showed either no identifiable posterior boundary of the choroid or a portion of the choroidal structure was missing.

The anterior boundary of the choroid in each image was defined as the hyper-reflective band corresponding to the RPE-Bruch's membrane complex. The posterior boundary was defined and based on the classification as follows: for group A, the outer limit of the CSI was used; for group B, the outer limit of the CSI was used where both SCS and CSI were visible in the image. Where only one of the two were identifiable, the posterior boundary was drawn at either the outer limit of the CSI or the inner limit of the SCS. For group C, the smooth band signifying the outer limit of the large choroidal vessels was used.

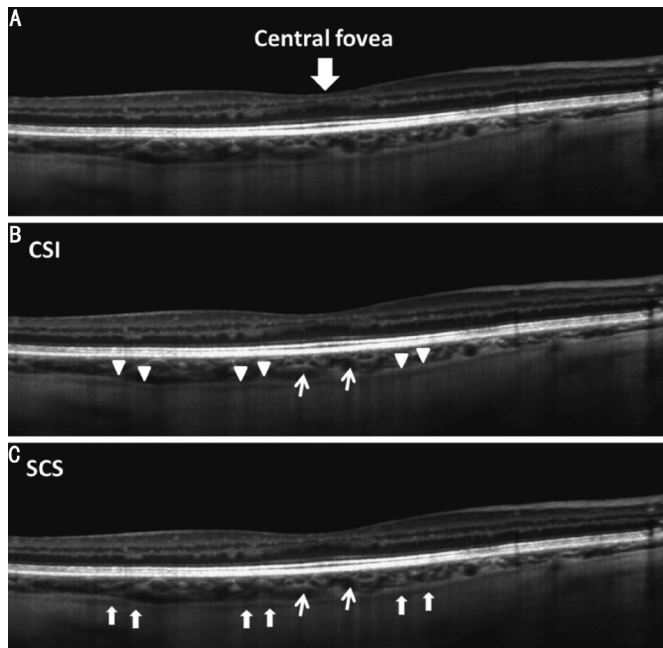


Figure 1 A single 9 mm horizontal line scan with enhanced depth imaging obtained from the right eye of a 55-year-old healthy male. A: The choroidal-scleral interface (CSI); B: Is indicated by a well demarcated hyper-reflective band (triangle heads) and the suprachoroidal space (SCS); C: Is indicated by the hypo-reflective band (arrows). The narrow arrows indicate the cross section of large choroidal vessels.

Measurement of Choroidal Thickness All EDI OCT images were classified and delineated using the proposed protocol by two masked expert observers (Boonarpa N and Stangos AN). In addition, observer Boonarpa N repeated the classification and measurement tasks one week later, masked from the previous measurements. The anterior and posterior boundaries of the choroid were manually delineated using Image J software version 1.45S (National Institutes of Health, USA). The ChT was then measured as the perpendicular distance between the anterior and posterior boundary at 500 μm intervals up to 3 mm nasal and 3 mm temporal from the foveal center using a program developed in MATLAB R2012a (The Mathworks Inc., Natick, USA). The total ChT was calculated from the average ChT from the 13 locations measured. The subfoveal ChT was used to represent the ChT at the foveal center.

Two evaluation iterations were performed: in the pilot study, the images from healthy volunteers were analyzed to test if the standardization methodology was valid. The second experiment was performed to evaluate whether the protocol was applicable for the management of disease represented by images from patients with diabetes.

Statistical Analysis Statistical analyses were performed using the Statistical Package for Social Scientists (SPSS) program version 20 (SPSS Inc., IBM, USA).

In order to determine the level of agreement between observers on the evaluation of the choroidal topographic

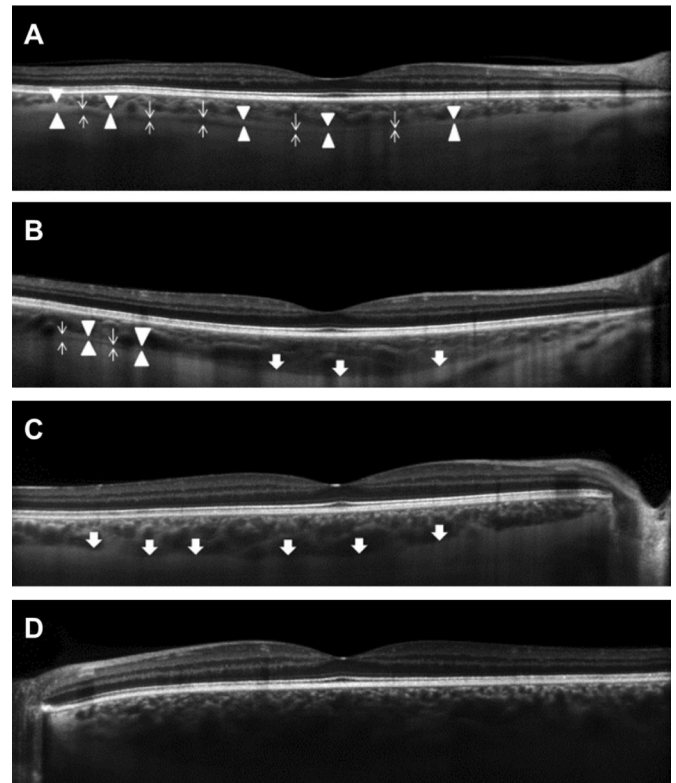


Figure 2 Example of EDI OCT image classifications categories. Group A (A), the choroidal outer boundary consists of more than 80% of the CSI (triangle heads) and the SCS (narrow arrows) across the length of the scan. Group B (B) consists of less than 80% of the CSI and the SCS across the length of the scan. Group C (C) consists of a smooth line between the outer limit of large choroidal vessels and the sclera (wide arrows) and ungradable (D) when the outer choroidal boundary is not identifiable on the scan.

appearances on EDI OCT scans, the Cohen's kappa coefficient (κ) was calculated (less than 0.20 signifies poor agreement, $\kappa=0.21-0.40$ fair, $\kappa=0.41-0.60$ moderate, $\kappa=0.61-0.80$ substantial, $\kappa=0.81-1.00$ almost perfect agreement)^[18].

Inter- and intra-observer agreements for the thickness measurements were shown using Bland and Altman plot^[19]. The coefficient of repeatability (CR) was defined as $1.96 \times$ standard deviation (SD) between two measurements. These analyses were done separately on 5 sets of images (*i.e.* group A, group B, group C, group agreed as ungradable and non-agreed images) for the total ChT and the subfoveal ChT. Intraclass correlation coefficient (ICC) was used to determine the reliability of the measurements. An ICC value below 0.40 represents poor agreement, 0.40-0.75 represents fair to good agreement and above 0.75 represents excellent agreement^[20]. A 5% level of significance was considered.

RESULTS

A total of 58 subjects (46 patients with diabetes and 12 healthy volunteers) were recruited in this study. The mean age of the 12 healthy volunteers (5 males) was 43.3 (± 12)y (range 28-67). The mean age of the 46 subjects with diabetes

Table 1 Summary of inter-observer agreements on the total and subfoveal choroidal thickness measurements

Inter-observer agreement	Total ChT			Subfoveal ChT		
	ICC (95%CI)	Mean difference (95%CI) (μm)	CR (μm)	ICC (95%CI)	Mean difference (95%CI) (μm)	CR (μm)
Group A	0.985 (0.873-0.996)	7.1 (4.1-10.2)	14.1	0.986 (0.965-0.994)	4.4 (-0.4-9.2)	22.2
Group B	0.963 (0.913-0.984)	5.8 (-3.5-15.0)	40.7	0.916 (0.778-0.967)	18.5 (2.7-34.3)	69.8
Group C	0.971 (0.912-0.990)	10.7 (-0.2-21.6)	41.4	0.959 (0.880-0.985)	15.1 (-1.0-31.2)	61.4
Overall	0.972 (0.944-0.985)	7.6 (3.4-11.9)	33.1	0.949 (0.900-0.972)	12.2 (5.2-19.2)	54.4
Non-agreement	0.964 (0.878-0.988)	15.7 (3.4-28.0)	49.9	0.918 (0.747-0.971)	27.4 (5.5-49.3)	89.2

ICC: Intraclass correlation coefficient; CI: Confidence interval; CR: Coefficient of repeatability; ChT: Choroidal thickness.

Table 2 Summary of intra-observer agreements on the total and subfoveal choroidal thickness measurements

Intra-observer agreement	Total ChT			Subfoveal ChT		
	ICC (95%CI)	Mean difference (95%CI) (μm)	CR (μm)	ICC (95%CI)	Mean difference (95%CI) (μm)	CR (μm)
Group A	0.996 (0.985-0.999)	2.9 (1.1-4.8)	8.8	0.989 (0.975-0.995)	2.0 (-2.4-6.4)	21.2
Group B	0.989 (0.973-0.996)	-4.2 (-9.3-1.0)	22.1	0.984 (0.961-0.993)	-4.5 (-13.0-4.1)	36.8
Group C	0.996 (0.991-0.998)	-0.5 (-4.4-3.4)	18.0	0.982 (0.958-0.992)	-0.6 (-10.7-9.5)	46.8
Overall	0.995 (0.991-0.997)	-0.3 (-2.4-1.8)	17.5	0.985 (0.975-0.990)	-0.8 (-5.1-3.6)	35.9
Non-agreement	0.981 (0.912-0.996)	6.3 (-4.9-17.4)	26.1	0.927 (0.686-0.985)	4.4 (- 21.3-30.0)	60.1

ICC: Intraclass correlation coefficient; CI: Confidence interval; CR: Coefficient of repeatability; ChT: Choroidal thickness.

(36 males) was 54.4 (±15)y (range 20-76). Eighty-two EDI OCT images from both eyes of the 46 subjects were included in this study. In this group, EDI OCT scans could not be obtained from one of the eyes of 10 patients due to poor fixation. On clinical examination, 24 eyes were graded with M1 diabetic maculopathy and 1 eye had M0.5 maculopathy^[6]. Five OCT scans passing through the fovea showed intraretinal fluid. There was no statistically significant difference in ChT measurements between the scans with maculopathy and without maculopathy ($P>0.05$, data not shown). The visual acuity (logMAR) was -0.01 (±0.11).

In the pilot study on 12 eyes of 12 healthy volunteers (one eye per subject), the inter- and intra-observer agreements on the choroidal posterior boundary classification were $\kappa=0.42$ and $\kappa=1$, respectively. The ICC for inter-observer agreement on the total ChT on the scans in which the image classification was agreed was 0.960 [95% confidence interval (CI), 0.684-0.994] and 0.992 (95% CI, 0.972-0.998) for intra-observer agreement.

This protocol was then applied to the 82 EDI OCT images of the 46 diabetic subjects. The inter-observer agreement on the image classifications was $\kappa=0.66$ (95% CI, 0.53-0.79; $P<0.001$). Both observers agreed on the classification of 63 EDI OCT scans: 24 scans (38.1%) were classified as group A, 22 (34.9%) as group B, and 17 (27.0%) as group C. The intra-observer agreement on the image classification was $\kappa=0.86$ -95% CI, 0.76-0.95; $P<0.001$ where 74 EDI OCT scans were given the same classification: 26 scans (35.1%) group A, 21 scans (28.4%) group B, 24 scans (32.4%) group C and 3 scans (4.1%) were ungradable.

There were excellent inter- and intra-observer agreements of ChT measurements in patients with diabetes on both, the total

ChT and subfoveal ChT, for scans that received the same classification from the observers. The inter-observer ICC values ranged from 0.963 to 0.985 with an overall ICC value of 0.972 (95% CI, 0.944-0.985) for the total ChT and from 0.916 to 0.986 with an overall ICC of 0.949 (95% CI, 0.900-0.972) for subfoveal ChT (Table 1). The ICC for intra-observer measurement agreement ranged from 0.989 to 0.996 with the overall ICC value of 0.995 (95% CI, 0.991-0.997) for the total ChT and 0.982 to 0.989 with the overall ICC of 0.985 (95% CI, 0.975-0.990) for subfoveal ChT (Table 2). The EDI OCT scans classified as group A showed greater reliability for both the total ChT and subfoveal ChT (as shown by the ICC value) than those EDI OCT scans containing less identifiable structures (groups B and C).

Figure 3 shows Bland and Altman plots of the inter-observer and intra-observer differences versus the mean of total ChT for each EDI OCT image classification. Figure 4 shows Bland and Altman plots^[19] of the inter-observer and intra-observer differences versus the mean of subfoveal ChT for each image classification. The inter-observer CRs for the total ChT in EDI OCT scans classified as group A, B and C were 14.1 μm, 40.7 μm and 41.4 μm respectively with an overall CR value of 33.1 μm. The intra-observer CRs for the total ChT were 8.8 μm, 22.1 μm and 18.0 μm for groups A, B and C respectively with an overall CR value of 17.5 μm. The inter- and intra-observer CRs of the subfoveal ChT were approximately 2 times higher than those of the total ChT in each image classification (Tables 1, 2).

DISCUSSION

Measuring the ChT has proven to be challenging, as there is a considerable variation in the transitional zone between the

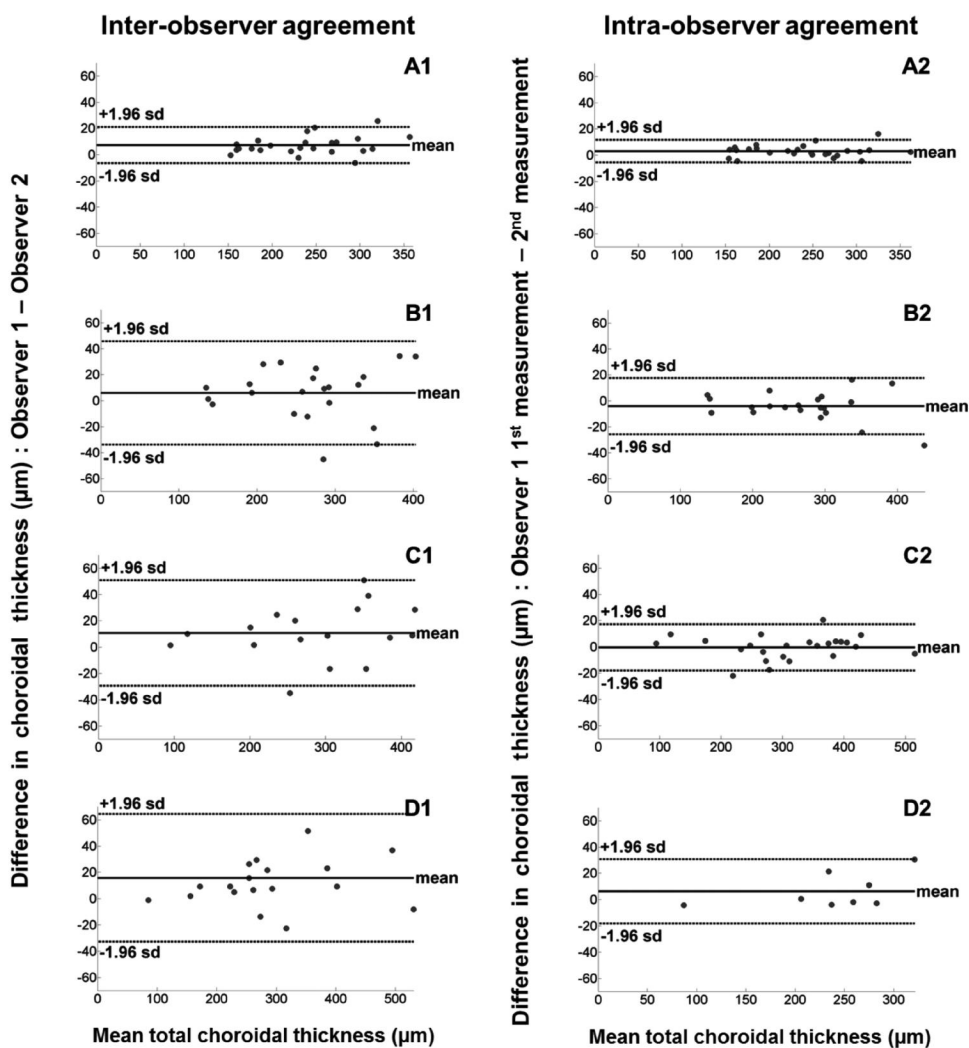


Figure 3 Bland–Altman plots showing inter–observer (right hand column) and intra–observer agreements (left hand column) with mean difference (thick line) and 95% limits of agreement (dashed lines) for the total ChT measurements by classification A1, A2: Group A; B1, B2: Group B; C1, C2: Group C; D1, D2: Non-agreement.

outer choroidal boundary and the sclera even in the absence of pathology. A clear standardized definition of the limits of the outer boundary of the choroid on EDI OCT images is needed in order to allow a comparison across clinical studies as this can affect the reliability of measurements, especially for those scans taken from diseased eyes.

To address this issue, we have developed a standardized protocol based on the presence and/or absence of the SCS and the CSI, seen as the hypo-reflective and the hyper-reflective bands respectively at the outer boundary of an EDI-OCT image. Using these criteria, we have classified the images into 4 groups: A, B, C and ungradable. To our knowledge this detailed descriptive definition of the outer boundary of the choroid has not been reported previously. We have demonstrated good agreement in grading the images by using the proposed protocol and excellent user concordance in evaluating the ChT on images taken from healthy eyes and those taken from eyes with diabetes. Additionally, although a single horizontal EDI OCT line scan passing through the center of the fovea was used in this

study, our standardized definitions of the choroidal outer boundaries could also be applied for the volumetric analysis of the choroid since the protocol has accounted for irregularities of the choroidal outer boundary.

The variation in the topographic appearances of the choroidal posterior boundary has been known to affect ChT measurements. An example of the variation of the topographic appearances was shown by Maul *et al*^[13], who graded the EDI OCT images obtained from glaucoma subjects using the criteria of presence or absence of CSI. Their results suggested a significant association between the variability in appearance of the choroidal outer boundary and the ChT measurement. The results presented in this study not only show an agreement with those presented by Maul *et al*^[13] but also suggest that the variability of the choroidal outer boundary affect the reliability of the total ChT and subfoveal ChT measurements. In particular, there was a relatively large variation in the choroidal measurement agreement found in the group of scans in which the choroidal outer boundary structure was less visible (groups B and C).

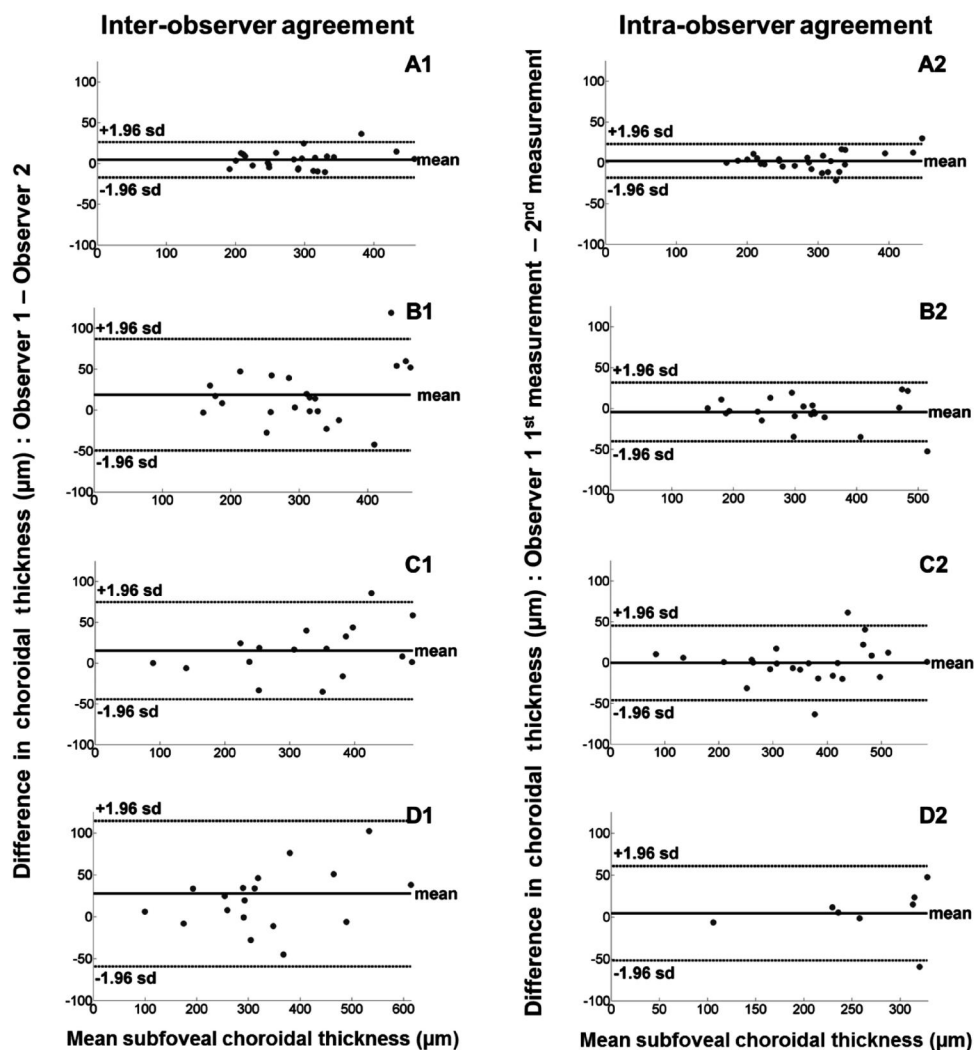


Figure 4 Bland–Altman plots showing inter–observer (right hand column) and intra–observer agreements (left hand column) with mean difference (thick line) and 95% limits of agreement (dashed lines) for ChT measurements at the foveal center by classification A1, A2: Group A; B1, B2: Group B; C1, C2: Group C; D1, D2: Non-agreement.

Other factors that may influence the ability to visualize the choroidal posterior boundary include patients' fixation and the type of commercial OCT instruments used. There is a wide variation in the reports: Using Cirrus OCT, Ho *et al*^[21] could measure the ChT in 90% of the scans while Manjunath *et al*^[22] could delineate the choroidal boundary from only 34 of 46 (74%) of the OCT scans. Using Heidelberg Spectralis OCT, previous reports have shown variations between 92% and 96% as reported by Kim *et al*^[23] and Mwanza *et al*^[24] respectively.

In order to be used in a clinical setting, manual ChT measurements require adequate inter- and intra-observer agreements. In healthy subjects, Spaide *et al*^[4] previously reported a high inter-observer correlation of 34 eyes from 17 healthy volunteers ($r > 0.90$). Rahman *et al*^[25] showed high intra-observer, inter-observer and intra-session correlations on ChT measurements. In subjects with diabetes, the inter-observer correlation of the ChT has been reported at 0.81 using Heidelberg Spectralis OCT^[26]. These authors, however, only reported the measurement agreement at the

central fovea whereas in our study we have used the entire length of the scan. Another important point to note is that the majority of the studies published report the ChT measurement reliability using Pearson's correlation coefficient^[4,22,25,26]. Pearson's correlation coefficient only illustrates the linear association of two variables but not the agreement between the measurements^[27,28] and thus, it would be inappropriate to use Pearson's coefficient. Inappropriate statistical methods used for assessing the reliability may be misleading and lead to unreliable conclusions. In this study we have used the ICC and the kappa coefficient, which are the most appropriate methods to measure the reliability of continuous and categorical data respectively^[20,27]. We have shown that higher measurement agreements can be achieved using our measurement protocol for both healthy eyes and eyes with diabetes (all ICC > 0.9).

CR has also been used to determine the agreement of the ChT measurement. A previous study has reported that the CR of manual caliper measurements on the subfoveal ChT in healthy eyes is 23.3 μm (95% CI, 18.7-27.9 μm) for

intra-observer and $>32.1 \mu\text{m}$ (95% CI, 30.0–4.9 μm) for inter-observer agreements [25]. In patients with chorioretinal diseases, the CRs were shown to increase from the normal range. This may suggest that the variability of ChT measurements increase as the choroidal outer boundary becomes less recognizable due to the changes in the ChT or retinal structures. The inter-observer CR values at the center of the fovea in patients with nonexudative AMD, exudative AMD, polypoidal choroidal vasculopathy (PCV) and CSCR ranged between 24–26 μm , 30–36 μm , 39–45 μm and 46–50 μm respectively [29]. We have shown that in patients with DR, the inter-observer CR at the central foveal ChT was 54 μm using our proposed measurement protocol. This result was comparable to that obtained by Sim *et al* [30] who reported the CR for inter-observer agreement on the subfoveal ChT was 53 μm . The inter-observer CR for the total ChT obtained using our measurement protocol, however, provided a much smaller CR value than that obtained by Sim *et al* [30] (33 μm vs 42 μm) which is an indication of a better agreement between observers for the total ChT.

The intra-observer CRs for ChT measurements in diabetic patients were generally smaller than the inter-observer CRs. The intra-observer CRs obtained were 18 μm for the total ChT and 36 μm for subfoveal ChT. These results agree with those of previous investigations on the ChT measurement in other retinal diseases, such as AMD and CSCR [29]. Although these intra-observer CRs were better compared to a previous report [30] (26 μm for total ChT and 48.3 μm for the subfoveal ChT), it is difficult to make a comparison between our CRs and those provided by the previous reports for several reasons: firstly, these reports did not take into account the topographical variation in the outer boundary of the choroid on EDI OCT images and secondly, the number of points measured and the methods used to measure the ChT were different. Our measurements include the extra vascular layers of the choroid into the measurements while other protocols may fail to include the extra vascular choroidal structure.

Our results have also shown that the CR values increased for both, the inter- and intra-observer measurements as the choroidal outer boundary becomes less identifiable (with the smallest in group A). This suggests a direct impact of the image qualities on the thickness measurements. Hence great care needs to be taken while interpreting the results of the studies that do not report image quality parameters at the outset. This can also have implications in obtaining meaningful results for example while comparing the ChT measurements pre- and post-treatment. In addition, automation techniques for the segmentation of the choroid are becoming an active research topic [31–33]. To evaluate the performance of these automatic techniques, the manual annotations by experts are usually used as a reference

standard. Thus, our standardized protocol can be used to study the reliability and accuracy of the automatic techniques.

In conclusion, we have introduced standardized definitions of the outer and inner boundaries of the choroid in EDI OCT images and we have demonstrated its significance in accurate measurements of ChT.

ACKNOWLEDGEMENTS

Foundation: Supported by Foundation for the Prevention of Blindness.

Conflicts of Interest: Boonarpha N, None; Zheng Y, None; Stangos AN, None; Lu H, None; Raj A, None; Czanner G, None; Harding SP, None; Nair –Sahni J, None.

REFERENCES

- 1 Luttj G, Grunwald J, Majji AB, Uyama M, Yoneya S. Changes in choriocapillaris and retinal pigment epithelium in age-related macular degeneration. *Mol Vis* 1999;5:35–38
- 2 Imamura Y, Fujiwara T, Margolis R, Spaide RF. Enhanced depth imaging optical coherence tomography of the choroid in central serous chorioretinopathy. *Retina* 2009;29(10):1469–1473
- 3 Vujosevic S, Martini F, Cavarzeran F, Pilotto E, Midena E. Macular and peripapillary choroidal thickness in diabetic patients. *Retina* 2012;32(9):1781–1790
- 4 Spaide RF, Koizumi H, Pozzoni MC. Enhanced depth imaging spectral-domain optical coherence tomography. *Am J Ophthalmol* 2008;146(4):496–500
- 5 Mansouri K, Medeiros FA, Marchase N, Tatham AJ, Auerbach D, Weinreb RN. Assessment of choroidal thickness and volume during the water drinking test by swept-source optical coherence tomography. *Ophthalmology* 2013;120(12):2508–2516
- 6 Fong AHC, Li KKW, Wong D. Choroidal evaluation using enhanced depth imaging spectral-domain optical coherence tomography in vogt-koyanagi-harada disease. *Retina* 2011;31(3):502–509
- 7 Fujiwara T, Imamura Y, Margolis R, Slakter JS, Spaide RF. Enhanced depth imaging optical coherence tomography of the choroid in highly myopic eyes. *Am J Ophthalmol* 2009;148(3):445–450
- 8 Reibaldi M, Boscia F, Avitabile T, Uva MG, Russo V, Zagari M, Bonfiglio V, Reibaldi A, Longo A. Enhanced depth imaging optical coherence tomography of the choroid in idiopathic macular hole: a cross-sectional prospective study. *Am J Ophthalmol* 2011;151(1):112–117
- 9 Fujiwara A, Shiragami C, Shirakata Y, Manabe S, Izumibata S, Shiraga F. Enhanced depth imaging spectral-domain optical coherence tomography of subfoveal choroidal thickness in normal Japanese eyes. *Jpn J Ophthalmol* 2012;56(3):230–235
- 10 Margolis R, Spaide RF. A pilot study of enhanced depth imaging optical coherence tomography of the choroid in normal eyes. *Am J Ophthalmol* 2009;147(5):811–815
- 11 Ding X, Li J, Zeng J, Ma W, Liu R, Li T, Yu S, Tang S. Choroidal thickness in healthy chinese subjects. *Invest Ophthalmol Vis Sci* 2011;52(13):9555–9560
- 12 Remington LA. Uvea. In Remington LA, ed. *Clinical Anatomy and Physiology of the Visual System* 3rd ed. Saint Louis: Butterworth-Heinemann;2012:40–60
- 13 Maul EA, Friedman DS, Chang DS, Boland MV, Ramulu PY, Jampel HD, Quigley HA. Choroidal thickness measured by spectral domain optical

- coherence tomography factors affecting thickness in glaucoma patients. *Ophthalmology* 2011;118(8):1571-1579
- 14 Branchini L, Regatieri CV, Flores-Moreno I, Baumann B, Fujimoto JG, Duker JS. Reproducibility of choroidal thickness measurements across three spectral domain optical coherence tomography systems. *Ophthalmology* 2012;119(1):119-123
- 15 Imamura Y, Iida T, Maruko I, Zweifel SA, Spaide RF. Enhanced Depth Imaging Optical Coherence Tomography of the Sclera in Dome-Shaped Macula. *Am J Ophthalmol* 2011;151(2):297-302
- 16 Younis N, Broadbent DM, Harding SP, Vora JR. Prevalence of diabetic eye disease in patients entering a systematic primary care-based eye screening programme. *Diabet Med* 2002;19(12):1014-1021
- 17 Sahni J, Stanga P, Wong D, Harding S. Optical coherence tomography in photodynamic therapy for subfoveal choroidal neovascularisation secondary to age related macular degeneration: a cross sectional study. *Br J Ophthalmol* 2005;89(3):316-320
- 18 Landis JR, Koch GG. The measurement of observer agreement for categorical data. *Biometrics* 1977; 33(1):159-174
- 19 Bland JM, Altman DG. Statistical methods for assessing agreement between two methods of clinical measurement. *Lancet* 1986;1 (8476): 307-310
- 20 Fleiss JL. Reliability of Measurement. *The Design and Analysis of Clinical Experiments* Hoboken, NJ, USA, John Wiley & Sons Inc.;1999: 1-32
- 21 Ho J, Branchini L, Regatieri C, Krishnan C, Fujimoto JG, Duker JS. Analysis of normal peripapillary choroidal thickness via spectral domain optical coherence tomography. *Ophthalmology* 2011;118(10):2001-2007
- 22 Manjunath V, Taha M, Fujimoto JG, Duker JS. Choroidal thickness in normal eyes measured using Cirrus HD optical coherence tomography. *Am J Ophthalmol* 2010;150(3):325-329
- 23 Kim M, Kim SS, Kwon HJ, Koh HJ, Lee SC. Association between choroidal thickness and ocular perfusion pressure in young, healthy subjects: enhanced depth imaging optical coherence tomography study. *Invest Ophthalmol Vis Sci* 2012;53(12):7710-7717
- 24 Mwanza JC, Hochberg JT, Banitt MR, Feuer WJ, Budenz DL. Lack of association between glaucoma and macular choroidal thickness measured with enhanced depth-imaging optical coherence tomography. *Invest Ophthalmol Vis Sci* 2011;52(6):3430-3435
- 25 Rahman W, Chen FK, Yeoh J, Patel P, Tufail A, Da Cruz L. Repeatability of manual subfoveal choroidal thickness measurements in healthy subjects using the technique of enhanced depth imaging optical coherence tomography. *Invest Ophthalmol Vis Sci* 2011;52(5):2267-2271
- 26 Querques G, Lattanzio R, Querques L, Del Turco C, Forte R, Pierro L, Souied EH, Bandello F. Enhanced depth imaging optical coherence tomography in type 2 diabetes. *Invest Ophthalmol Vis Sci* 2012;53(10): 6017-6024
- 27 Bartko JJ. Measurement and reliability: statistical thinking considerations. *Schizophr Bull* 1991;17(3):483-489
- 28 Bland JM, Altman DG. Measuring agreement in method comparison studies. *Stat Methods Med Res* 1999;8(2):135-160
- 29 Kim JH, Kang SW, Kim JR, Kim SJ. Variability of subfoveal choroidal thickness measurements in patients with age-related macular degeneration and central serous chorioretinopathy. *Eye (Lond)* 2013;27(7):809-815
- 30 Sim DA, Keane PA, Mehta H, Fung S, Zarranz-Ventura J, Fruttiger M, Patel PJ, Egan CA, Tufail A. Repeatability and reproducibility of choroidal vessel layer measurements in diabetic retinopathy using enhanced depth optical coherence tomography. *Invest Ophthalmol Vis Sci* 2013;54(4): 2893-2901
- 31 Lu H, Boonarpa N, Kwong MT, Zheng Y. Automated segmentation of the choroid in retinal optical coherence tomography images. *Conf Proc IEEE Eng Med Biol Soc* 2013;2013: 5869-5872
- 32 Hu Z, Wu X, Ouyang Y, Ouyang Y, Sadda SR. Semiautomated segmentation of the choroid in spectral-domain optical coherence tomography volume scans. *Invest Ophthalmol Vis Sci* 2013;54(3):1722-1729
- 33 Zhang L, Lee K, Niemeijer M, Mullins RF, Sonka M, Abramoff MD. Automated segmentation of the choroid from clinical SD-OCT. *Invest Ophthalmol Vis Sci* 2012;53(12):7510-7519